Seismic Fragility Functions via Nonlinear Response History Analysis

Konstantinos Bakalis[1] and Dimitrios Vamvatsikos[2]

Abstract: The estimation of building fragility, i.e. the probability function of seismic demand exceeding a certain limit state capacity given the seismic intensity, is a common process inherent in any seismic assessment study. Despite this prolific nature, the theory and practice underlying the various approaches for fragility evaluation may be opaque to their users, especially regarding the handling of demand and capacity uncertainty, or the generation of a single fragility curve for multiple failure conditions, using either an intensity measure or engineering demand parameter basis. Hence, a comprehensive guide is provided that compiles all necessary information for generating fragility curves of single structures based on the results of nonlinear dynamic analysis. Although various analysis methods are discussed, Incremental Dynamic Analysis is invoked to clearly outline different methodologies that rely either on response parameter or intensity measure ordinates. Step-by-step examples are presented for each case, both under a deterministic and an uncertain limit state capacity framework, using limit states that range from simple structural damage to the global collapse of the structure.

CE Database subject headings: Seismic fragility; Earthquakes; Performance evaluation;

Author Keywords: performance-based earthquake engineering; incremental dynamic analysis; uncertainty; fragility; demand; capacity;

---

[1] PhD Student, School of Civil Engineering, National Technical Univ. of Athens, Greece (corresponding author). E-mail: kbakalis@mail.ntua.gr

[2] Assistant Professor, School of Civil Engineering, National Technical Univ. of Athens, Greece. E-mail: divamva@mail.ntua.gr

Introduction

Fragility is a versatile term employed throughout earthquake engineering to describe the susceptibility of a structure (or part of a structure) to seismic damage. Its estimation can be based on a variety of empirical (Rossetto et al. 2014), numerical (D'Ayala et al. 2015) or expert opinion data (Jaiswal et al. 2011), and their combinations, using various methodologies that range from pure statistical processing of existing data (Lallemant et al. 2015; Noh et al. 2015) to computational static and dynamic procedures that generate new data from scratch (D'Ayala et al. 2015; Rossetto and Elnashai 2005; Shinozuka et al. 2000). The first type features the generation of "empirical fragility curves" (ATC 1985), typically for classes of structures, and will not be dealt with herein, whereas the second refers to the so-called "analytical fragility curves", derived either for a class of similar structures (Silva et al. 2014), or for a specific one for which a custom structural model has been formulated. The latter case, i.e., the analytical derivation of structure-specific fragilities is the main subject of this study. Note that the analytical designation may seem misleading, given that they are a product of numerical analysis rather than some analytical equation; yet, the connection to "analysis" compared to "statistical fitting" is a more apt distinction to understand the term. The field of application for fragility is so wide that one should begin by attempting to narrow it down and focus on a very specific (yet widely applicable) definition. Henceforth, a building fragility is defined as a probability-valued function of a building's seismic demand (D, i.e. a response parameter of interest, as determined by numerical analysis) at a given level of seismic intensity, exceeding an associated capacity threshold (C, e.g. defined by pertinent assessment guidelines such as ASCE41-06 (ASCE 2007)) that signals violation of a limit state (LS) of interest. A fragility function is thus parametrised by one or more scalar intensity measures (IMs) that characterise the seismic intensity (e.g. peak ground acceleration (PGA), first-mode spectral acceleration ($S_a(T_1)$), etc.).

Of particular interest, hereafter, is the case of a single *IM*, for the so-called fragility curves (versus e.g. surfaces for two *IMs*).

Although a fragility curve corresponds to a single limit state, it actually splits the entire event space into two complementary events, namely "*LS* exceeded" and "*LS* not exceeded", often associated with specific (distinct) damage states (i.e. DS_i, DS_{i+1}) in the literature (e.g. light versus moderate damage). Be aware that "exceeding" a state may sometimes be linguistically construed as being better to it; still, in the fragility context "exceedance" and "violation" of a limit state are considered interchangeable. Traditionally, the "fragility" term has been used to describe conceptually different entities, such as *component* damage conditioned on engineering demand parameters (*EDPs*, e.g. inter-story drift or peak floor acceleration) and *building/system* damage conditioned on seismic intensity (FEMA 2012; Nielson and DesRoches 2007a; b; Porter et al. 2006). There are advantages to be had when looking at limit states of specific components (rather than aggregating to the whole structure), especially when looking at the estimation of repair cost, downtime (Goulet et al. 2007; Miranda and Aslani 2003; Mitrani-Reiser 2007), or even casualties. In this paper, however, the "fragility" term is strictly associated with the system (building) fragility conditioned on the seismic intensity.

The reason why fragility is such an important step in almost every seismic-related study is uncertainty (Gidaris et al. 2017). There is uncertainty on the structural capacity as well as on the associated demand. A good way to understand the significance of fragility is to think of a purely deterministic scenario, where a simple comparison between capacity and demand would provide a probability of violating (or exceeding) the limit state under investigation equal to "1" for the case that the event $[D > C]$ is satisfied, and "0" otherwise. Inevitably, the fragility curve given the *IM* becomes a step function, changing from "0" to "1" at the *LS* capacity. To incorporate uncertainty on a code-basis, traditional design or assessment, safety checks are performed using pertinent safety factors that are calibrated to correspond to a given probability level, for both capacity and demand. The problem is that they provide a single "yes or no" answer, while the inclusion of safety factors only means that the "yes or no" answer is valid at the single pre-calibrated safety factor probability level. Instead, when uncertainty is fully taken into account for demand and/or capacity, the well-known S-shaped fragility curve is attained. The latter provides the probability that demand exceeds capacity (i.e. $D > C$) at all possible intensity levels, or in other words summarises the results of all possible single-level safety checks into a continuous function.

A good way to look at the estimation of fragilities is by realising that it is simply a method to propagate uncertainty from the intensity measure to the limit state check/assessment of the structure (Ellingwood and Kinali 2009). In general, as Bazzurro et al. (2006) correctly observed, fragilities are actually characterised by a central (median) *IM* capacity value and an associated dispersion. They can be thought and used exactly as the cumulative distribution function (CDF) of the building-specific limit state *IM* capacity. For instance, if a future earthquake event reaches a certain *IM* value, information on the probability of pushing the structure to a limit state is immediately provided. Most telling, if the seismic intensity equals the median *IM* capacity, there is a 50% chance that the earthquake violates the associated limit state.

Herein, the derivation of seismic fragility using nonlinear response history analysis methods is discussed. Due to the delicate nature of the topic under discussion, the authors feel inclined to state that this manuscript does not attempt to offer new results. Instead, it aims to provide a carefully structured discussion of how fragility can/should be estimated via several acceptable approaches so as to provide consistent results with any and all of them.

Formal Definitions

The notion of fragility is intimately tied to the idea of the *intensity measure*. An intensity measure is a quantity indicative of the severity of the ground motion at a given site and is meant to act as an interface between seismology and structural engineering. Typically, *IM* is a scalar variable, usually the $S_a(T_1)$ or even the *PGA*, for which there are ground motion prediction equations available, such that the hazard curve generation is possible. In this view of the performance-based assessment problem, seismologists would model any faults causing earthquakes that may affect the site under investigation, and summarise all information into a single hazard curve (or hazard surface in the case of a vector, Bazzurro and Cornell (2002)) representing the mean annual frequency (MAF) λ of exceeding certain levels of seismic intensity. Hazard curves are computed via probabilistic seismic hazard assessment (PSHA), whereby the myriads of possible earthquake scenarios are aggregated to achieve what is essentially a probabilistic *IM* distribution for the site under investigation. Structural engineers are typically expected to pick up the work at this point, functioning independently from seismologists, by estimating the distribution of structural response (typically characterised by pertinent *EDPs*, Bazzurro et al. (1998)), damage or loss that the structure of interest may experience, should it be subjected to given values of the *IM*. Ultimately, the *IM* becomes the single conduit to circulate information between seismologists and engineers, easing (although sometimes oversimplifying) communication considerably.

In an attempt to fully characterise a structure, engineers go one step further setting up *limit states* that allow discretising the continuous level of damage into discrete *damage states*, each with distinct consequences to the structure, its components or inhabitants. Associating each *DS* (or *LS*) with a desired (maximum acceptable) MAF of exceedance forms pairs known as performance objectives/targets that have an actual meaning for the operability of the structure itself, thus translating the engineering aspect of *EDPs* to something that actually makes sense even to non-engineers. Definition of each *LS* is achieved by assigning threshold (limiting or capacity) values for one or more *EDPs* whose exceedance triggers the limit state violation and brings the structure into a higher *DS*. In sight of the above, the *fragility curve* can be viewed as the summary of all structural analysis results, conditioned on the *IM*. Formally, it is defined as the probability function of violating a certain limit state given the value of the earthquake intensity measure. It is essentially a function of the intensity measure that may be expressed as

$$F_{LS}(IM) = \mathrm{P}\left[LS \text{ violated} \mid IM\right] = \mathrm{P}\left[D > C \mid IM\right], \quad (1)$$

where the second form assumes that *LS* violation is defined through a single *EDP* with demand *D* and limit state capacity *C*. In this case, fragility may be evaluated using either *EDP* or *IM* demand ordinates versus their associated capacities EDP_C and IM_C, respectively. Thus, equivalently to Eq. (1) the following expressions apply:

$$F_{LS}(IM) = \mathrm{P}\left[EDP > EDP_C \mid IM\right] \quad (2)$$

$$F_{LS}(IM) = \mathrm{P}\left[IM > IM_C\right] \quad (3)$$

Note that there are cases in the literature where fragility is expressed as $[D \geq C \mid IM]$ rather than $[D > C \mid IM]$, thus implying that in the rare case where capacity and demand are identical, the first signals violation while the second does not. This is mainly a matter of definition with respect to "exceedance" and "violation", and is generally not a real issue with continuous distributions, since $\mathrm{P}[D=C \mid IM]$ either equals zero or tends to zero, as the number of data points grows.

Customarily, a fragility curve is associated with two basic properties. First, at zero intensity, the probability of exceedance is zero. This is intuitive and needs no further explanation. Second, as *IM* approaches infinity, the very same probability should approach one. This seems natural as well and should be assured for any *IM* that properly corresponds to seismic intensity, although it is conceivable that some particularly bad *IM* choices would not possess this basic property. Take for instance the bracketed duration (e.g., $D_{5\text{-}75}$); quite often records of large duration are recorded at very large distances to subduction zones; then, higher duration correlates with lower intensities and thus a negative correlation coefficient between $S_a(T_1)$ and $D_{5\text{-}75}$ is often proposed (Bradley 2011). A third property is often assumed, namely that of monotonicity, or, in other words, that the function F_{LS} is strictly increasing. This is not a strict requirement according to the general definition via Eq. (1) or (2), although it is plausible that there may be a range of intensities where a structure may experience lower probabilities of limit state exceedance, compared to a lower intensity level. For example, Vamvatsikos and Cornell (2004) have observed such ranges of response, but for specific ground motions only; never for entire sets of records. Such occurrences in the entire set of analysis may be a sign of an insufficient *IM* or of inadequate ground motion sampling. Therefore, they should be carefully investigated whenever they appear. Nevertheless, as we expand our experiences with engineering structures, the possibility of such valid occurrences happening should not be discounted. In the general case though, it is safe to take monotonicity for granted, which enables the definition of fragility as the CDF $F(\cdot)$ of the structure's limit state capacity in terms of *IM* as implied by Eq. (3).

Definition via the Total Probability Theorem

A reader well-versed in Performance-Based Earthquake Engineering (PBEE) would recognise the central use of fragility in almost every aspect of analysis or design (Deierlein et al. 2003; Moehle and Deierlein 2004; Wen and Ellingwood 2005). The PBEE framework, originally developed by Cornell and Krawinkler (2000) for the Pacific Earthquake Engineering Research (PEER) Centre, serves as an alternative to the well-established Load and Resistance Factor Design, where the former can assess performance based on the MAF of decision variables (*DV*) similar to casualties, monetary loss and down time. To perform such an estimation, continuous damage measures (*DM*, e.g. concrete cracking and spalling), or usually discrete damage states, must be defined based on appropriate *EDPs* (e.g. roof displacement, drift), associated with ground motions at a range of *IM* levels [in terms of, e.g., *PGA* or $S_a(T_1)$] whose MAF is determined by the seismic hazard function $\lambda(IM)$. The entire PBEE methodology is summarised as an application of the total probability theorem as

$$\lambda(DV)=\int_{DM}\int_{EDP}\int_{IM} G(DV \mid DM)\left|\mathrm{d}G(DM \mid EDP)\right|\left|\mathrm{d}G(EDP \mid IM)\right|\left|\mathrm{d}\lambda(IM)\right|, \tag{4}$$

where $G(x\mid y)=\mathrm{P}(X>x \mid Y=y)$ is the conditional complementary cumulative distribution function (CCDF) of a random variable X given the value y of another random variable Y.

Changing the order of integrations on Eq. (4) provides interesting intermediate results, as nicely put by Miranda and Aslani (2003). Integrating the *IM* first, provides the MAF of the remaining variables, i.e. “hazard curves”. For instance, integrating the last two terms over *IM* provides $\lambda(EDP)$, or *EDP*-hazard (e.g. the drift hazard of Jalayer (2003)). On the other hand, if the *IM* conditioning is preserved, what we get is fragility or vulnerability curves. Integrating out *EDP*, considering that *DM* is discretised into multiple DS_i, provides fragility curves $\mathrm{G}(DS_i \mid IM)$. Integrating out *DM* (or DS_i) provides the vulnerability function $\mathrm{G}(DV \mid IM)$. Generally, “vulnerability” refers to measurements of loss (i.e. casualties, monetary loss, downtime) and should by no means be considered interchangeable to “fragility” that is strictly a measurement of probability (Porter 2015). Thus, equivalently to Eq. (4) $\lambda(DV)$ may also be expressed as:

$$\lambda(DV)=\int_{DM}\int_{IM} G(DV \mid DM)\left|\mathrm{d}G(DM \mid IM)\right|\left|\mathrm{d}\lambda(IM)\right| \tag{5}$$

$$\lambda(DV)=\int_{IM} G(DV \mid IM)\left|\mathrm{d}\lambda(IM)\right| \tag{6}$$

In some sense, although they appeared much earlier (e.g. in the nuclear industry, Kennedy and Ravindra (1984)), fragility curves can be viewed as an intermediate product of a PEER-like framework to estimate the probability of violating a certain limit state or damage state given the level of ground motion intensity.

Fragility may also be formulated in an alternative, yet more explicit, way through an alternative application of the total probability theorem. Bearing in mind that the *LS* term now refers to the associated *LS* violation, fragility can be expressed in the domain of a continuous *EDP* variable as

$$F_{LS}(IM) = \mathrm{P}[LS \mid IM] = \int_{EDP} \mathrm{P}[LS \mid EDP(IM)]\, f(EDP \mid IM)\, \mathrm{d}EDP\,, \tag{7}$$

where $f(x \mid y)$ is the probability density function (PDF) of a random variable X given the value y of another random variable Y. Applying the total probability theorem one more time to incorporate an additional level of integration over the intensity measure in order to account for the probability of occurrence for earthquakes of varying intensity, the MAF of *LS* violation is recovered as:

$$\lambda(LS) = \int_{IM} \left[\int_{EDP} \mathrm{P}[LS \mid EDP]\, f(EDP \mid IM)\, \mathrm{d}EDP \right] \left| \frac{\mathrm{d}\lambda(IM)}{\mathrm{d}IM} \right| \mathrm{d}IM \tag{8}$$

Eq. (8) is essentially identical to the PEER equation (Eq. (4)) provided that *DV* and *DM* are treated as index functions, which means that either of those variables becomes “1” when a certain *DM* or *LS* is exceeded, and “0” otherwise. Note that $\mathrm{d}\lambda(IM)/\mathrm{d}IM$ is the mean annual rate density of seismic intensity, or in other words the equivalent of PDF for rates. Applying any of the aforementioned equations may seem rather complex at first glance; however, such expressions are often evaluated numerically by discretising. For instance, partitioning the entire *EDP* range into N_{bin} bins of equal width ΔEDP, Eq. (7) can be realised through the sum of the individual probability products for the $[LS|EDP_i(IM)]$ and $[EDP_i|IM]$ events:

$$F_{LS}(IM) = \mathrm{P}[LS \mid IM] = \sum_{i=1}^{Nbin} \mathrm{P}[LS \mid EDP_i(IM)]\, \mathrm{P}[EDP_i \mid IM]\, \Delta EDP \tag{9}$$

While this integration (or summation) seems straightforward, there are many ways to estimate this deceptively tricky quantity. They are mostly affected by (a) the *EDP*|*IM* estimation methodology, (b) the uncertainties included, (c) whether the estimation is direct

(*EDP*-based, Eq. (2)) or indirect (*IM*-based, Eq. (3)), and (d) the integration approach, namely numerical or analytical via the typical lognormal assumptions on the various random parameters. The next few sections discuss these issues.

EDP-IM relationship

In the structural analysis context, each dynamic analysis provides a single pair of *IM* and (demand) *EDP* values. In view of the uncertainties involved, multiple analyses on a considerable number of ground motion records are required for every level of seismic intensity considered. There are many ways to group the aforementioned pairs in order to adequately characterise the *EDP-IM* space and estimate seismic demand, e.g. single-stripe (Jalayer 2003), multi-stripe (Jalayer 2003; Jalayer and Cornell 2009), cloud (with or without record selection and scaling, Jalayer 2003; Mackie and Stojadinovic 2001; Padgett and DesRoches 2008), or IDA (Vamvatsikos and Cornell 2002).

Since all analysis results are conditioned on values of the *IM*, it is mandatory that the *IM* contains all necessary information to make the analysis results insensitive to any other seismological variables, such as magnitude, distance or epsilon. This implies that when structural analysis is performed under a suite of ground motion records scaled to a given *IM* level, the estimated probabilistic distribution of the response does not depend on any seismological parameter. This is the well-known requirement of *IM* sufficiency (Luco and Cornell 2007). For example, *PGA* is known to be a relatively insufficient *IM*, unless short period structures subject to low levels of intensity are concerned. $S_a(T_1)$ has been shown to be an adequate choice for assessing first-mode dominated structures subject to far-field earthquakes (Shome et al. 1998) as long as excessive scale factors are not employed (Luco and Bazzurro 2007). Accounting for higher and/or elongated mode contributions has been shown to provide *IMs* with adequate sufficiency for near-field excitations, tall structures, collapse and loss assessment (Cordova et al. 2001; Eads et al. 2016; Kazantzi and Vamvatsikos 2015; Kohrangi et al. 2016; Tothong and Cornell 2008; Tsantaki et al. 2017). Alternatively, one may choose to employ sets of ground motions that account for the anticipated effect of seismological parameters at each level of an insufficient *IM*, rather than a single set across all intensities, at the cost of forfeiting independence from lower-level seismological information. For example, accounting for the distribution of epsilon at each level of *IM* has been shown to significantly improve the ability of S_a to lower/remove bias with respect to spectral shape in the prediction of structural response (Baker and Cornell 2006).

Without avoiding a bit of an authors' bias, fragility can best be understood in the realm of IDA (Vamvatsikos and Cornell 2002), where "failure" can easily be traced on a record-to-record basis. In brief, this procedure subjects a structural model to a set of records scaled to multiple levels of *IM*, in order to obtain the recorded *EDPs*, and thus the resulting (*EDP*, *IM*) points that are interpolated to form continuous IDA curves in the *EDP-IM* space. Fig. 1(a) presents the associated IDA curves (maximum inter-storey drift ratio $\theta_{\max}$ versus $S_a(T_1)$) for a 12-storey reinforced concrete frame building (see Kazantzi and Vamvatsikos (2015) for details), using the FEMA P-695 far field ground motion set (FEMA 2009). This is a modern, code-conforming, symmetric-plan, perimeter moment-resisting-frame, corresponding to seismic design category 'D' (FEMA 2009), modelled as a two-dimensional frame with fundamental period T_1=2.14s having both material and geometric nonlinearities. The PDFs (*EDP*|*IM* and *IM*|*EDP*) for an arbitrarily chosen *EDP* and *IM* level, are also provided to illustrate the inherent variability of the demand/capacity estimation problem. Both the horizontal (*EDP*|*IM*) and the vertical (*IM*|*EDP*) stripes are a direct result of the record-to-record randomness only, under the assumption that a fixed (i.e. deterministic) value of *EDP* capacity governs a certain damage state on the structure. For the case of IDA, the probability of exceeding a prescribed *EDP* limitation may thus be evaluated on the entire *EDP-IM* plane, using either of the respective ordinates (*EDP*, *IM*).

Other options to IDA are, for example, the cloud analysis, whereby a set of (scaled or unscaled) records appearing at arbitrary non-identical *IM* levels is used to obtain the *EDP-IM* relationship, and the stripe analysis that employs records scaled to various degrees to match the desired *IM* level(s) as shown in Fig. 1(b). Whenever a sufficient number of stripes is available, a multi-stripe analysis can be treated in more or less the same way as IDA. For cloud analysis, or in cases of few stripes, some form of regression is typically required to achieve a continuous representation of the distribution of *EDP*|*IM* for all *IM* levels of interest, which is normally performed through the well-known power-law approximation, as presented by Cornell et al. (2002)

$$EDP(IM) = E\hat{D}P(IM)\varepsilon = aIM^{b}\varepsilon\,, \tag{10}$$

where b is the slope in log-space, ln(a) the intercept, while ε is a lognormal random variable with unit median and a logarithmic standard deviation $\sigma_{\ln\varepsilon}$. The latter is interpreted as the constant dispersion of *EDP*|*IM*, which can be applied locally or globally, depending on how the fitting of Eq. (10) is performed. Often enough, assuming adequate points are available, local fitting provides higher fidelity as Eq. (10) is hardly capable of globally representing the richness of dynamic response shown in Fig. 1(a).

Sources of Fragility Uncertainty

Fragility is an inherently uncertain quantity subject to multiple sources of both aleatory and epistemic uncertainty (Ellingwood and Kinali 2009; Der Kiureghian and Ditlevsen 2009). They may be summarised as: (a) Record-to-record variability in the *IM-EDP* relationship, due to natural randomness of ground motions. This is directly related to the choice of the *IM*, in the sense that a more efficient *IM* would by definition produce lower variability, thus requiring fewer records to provide the same level of confidence on the prediction of the *EDP-IM* distribution. (b) Model-type uncertainty (e.g. Zeris et al. (2007)), referring to our imperfect modelling capabilities especially considering that simplified models are typically employed for computational efficiency reasons. (c) Model-parameter uncertainty (e.g. Dolsek 2009; Liel et al. 2009; Schotanus et al. 2004; Vamvatsikos and Fragiadakis 2009), due to incomplete knowledge or actual randomness in the model properties (e.g. strength, ductility, mass, stiffness). (d) Method-related uncertainty, due to imperfect methodology (e.g. a bad regression, an insufficient *IM*, or a deficient analysis approach, such as using nonlinear static analysis for a tall building (Fragiadakis et al. 2014). This should be avoided as much as possible. (e) Limit state capacity uncertainty, due to unknown or random *EDP* thresholds resulting from experiments or expert judgement. Of the above, (a) is purely aleatory, (b) and (d) are epistemic, while (c) and (e) may be either one or (usually) both leaning towards aleatory when a new (and yet unbuilt) structure is concerned, versus a combination of both when an existing structure is assessed.

In general, (a) is well captured by any of the aforementioned methods of analysis if an adequate number of records is employed. All other sources of uncertainty may invariably introduce both variability (i.e. increased dispersion) and bias (i.e. a shift in the central value). While the former is unavoidable, and guidelines have attempted to offer some standard or placeholder values for associated additional dispersions (FEMA 2012), the latter should be avoided as much as practically possible. Its effect is simply detrimental to the quality of assessment itself. This assumption of zero bias, but only added variance due to uncertainty, is referred to as the “first-order” assumption (Cornell et al. 2002).

Single-EDP Limit States

A single *EDP* is often employed to capture the functional state of a structure. This is the classic scenario encountered in the literature whereby estimation can be performed following strategies that rely either on *EDP* or *IM* ordinates, using either a deterministic or a probabilistic (i.e. uncertain) *EDP* capacity, and employing approximate closed-form solutions or the numerical integration of Eq. (9) via a Monte Carlo Simulation (MCS). Note that although IDA is hereafter invoked to outline the aforementioned fragility estimation procedures, fragility should by no means be tied to IDA, as alternative strategies (e.g. "cloud" and "stripe") may also be used to define the *EDP-IM* relationship. IDA is just a very convenient and thorough way of taking us there.

Deterministic EDP capacity

EDP-basis estimation

A general expression on the probability of violating a limit state for a given earthquake intensity is already given through Eq. (1). The aforementioned equation takes its simplest form when a single limiting EDP_C value is considered, i.e. assuming that there is no uncertainty in its definition. This is a very popular procedure among research and practicing engineers due to the simplicity it offers, as we are essentially looking for earthquake events that overcome the aforementioned capacity at the given seismic intensity. Hence, for any given (horizontal) stripe of analysis results (Fig. 1(a)), the probability of exceedance can be estimated through the sum of those events over the number of records (N_{rec}) used for the nonlinear dynamic analyses. In other words, to evaluate the formal integral of Eq. (7), or the sum of Eq. (9), instead of having to discretise the *EDP* space into bins of equal width, MCS is performed using a sample of N_{rec} equiprobable records:

$$F_{LS}(IM) = \mathrm{P}\left[EDP > EDP_C \mid IM\right] = \frac{\sum_{j=1}^{Nrec} \mathrm{I}\left[EDP^j > EDP_C \mid IM\right]}{N_{rec}} \qquad (11)$$

$\mathrm{I}(\cdot)$ is an index function that becomes “1” when the argument is true and “0” otherwise. This is the so-called *EDP*-basis or *given-IM* seismic fragility estimation, also known as *horizontal statistics* procedure (kudos to H. Krawinkler for the term (Zareian et al. 2004)). These definitions stem from the fact that the probability of exceedance estimation is performed on a stripe-basis, conditioned on the seismic intensity. Fig. 2(a) presents the entire set of IDA curves featuring the stripes at 0.2g, 0.4g and 0.6g of first mode spectral acceleration. A median limiting capacity (i.e. EDP_C) of $\theta_{\max}$=2% is chosen to illustrate the sequence of steps for the probability estimation. Considering the capacity of the *EDP* deterministic makes the seismic fragility estimation a rather trivial task. Take for instance the 0.2g *IM* level, where 3 out of the 44 records considered overcome the prescribed *EDP* capacity, thus resulting to a probability of exceedance equal to 3/44= 0.068. The probability of exceedance estimation for a number of *IM* levels spanning the entire *IM* space of interest is depicted on Fig. 2(b). The triangular data points are the direct result of Eq. (11), with the filled markers referring to the *IM* levels shown in Fig. 2(a). It is also customary that the discrete (in terms of *IM*) probability data points are summarised back to a continuous lognormal CDF (a fact that will be exploited extensively in later sections), or simply connected by linear segments to form an empirical distribution estimate. For a lognormal fit, the median (μ) as well as the dispersion (β, Fig. 2(b)) can be estimated using the 16%, 50% and 84% *IM* percentiles, the moment method or a maximum likelihood approach (Baker 2015). In other words, considering the *EDP* capacity as deterministic implies that the dispersion (and thus the slope) of the fragility curve is affected by the aleatory randomness only.

IM-basis estimation

An alternative to the *EDP*-basis procedure is the so-called *IM*-basis methodology, also known as *given-EDP* or *vertical statistics* (again an H. Krawinkler term (Zareian et al. 2004)) approach. This approach attains its simplest expression through Eq. (3), and may also be translated into the following empirical estimate of a CDF when a finite number (N_{rec}) of dynamic time history analyses has been employed each scaled to the level of IM_C^j (j=1…N_{rec}) to produce response equal to EDP_C:

$$F_{LS}(IM) = \mathrm{P}[IM > IM_C] = \frac{\sum_{j=1}^{Nrec} \mathrm{I}\left[IM > IM_C^j\right]}{N_{rec}} \tag{12}$$

In this case, the *IM* ordinates are employed to derive the associated seismic fragility curve. Under the assumption that the *EDP* capacity is represented by a single discrete value (i.e. deterministic approach), a vertical cut on the $\theta_{\max}$ of interest provides the single-record *IM* capacities. Bearing in mind that IM_C is an inherently probabilistic quantity, several records and IM_C^j values are required to obtain the entire fragility curve. The algorithm is pretty similar to the deterministic *EDP*-basis approach, only this time the probability of exceedance is estimated through the number of records that *do not* overcome the prescribed *IM* level (see also the vertical stripe on Fig. 1(a)). The latter remark is customarily harder to digest since the points of interest are found below the prescribed *IM* level. This is probably a visual orientation problem, as one would try to figure out values (i.e. demands) that exceed a limiting capacity, while in this case there is a single demand (i.e. a horizontal line at the prescribed *IM* level) to compare against multiple capacities along the vertical stripe: IM_C^j values found below the horizontal line signal exceedance of the limit state. Fig. 3(a) presents the *IM* capacities conditioned on the 2% inter-storey drift limit on the associated IDA curves. In a similar manner to the *EDP*-basis methodology, three *IM* levels, namely 0.2g, 0.4g and 0.6g of $S_a(T_1)$, are used to illustrate the probability of exceedance estimation. For the 0.2g of seismic intensity, only three records fail to deliver a better capacity, thus resulting to a 3/44=0.068 probability, which is fully consistent with the *EDP*-basis estimation (see also the discussion from Vamvatsikos & Cornell (Vamvatsikos and Cornell 2004) on the "equivalency" of *x*% *EDP*|*IM* and (1-*x*)% *IM*|*EDP* distributions). The discrete probabilities are illustrated on Fig. 3(b) for every seismic intensity considered, along with the associated fitted lognormal curve.

Global Instability

As much as the *EDP* and *IM*-basis approaches seem to agree for limit state capacities found on the ascending non-flat branch of IDA curves, there is an interesting discussion regarding their applicability for limit points that fall within the global instability region. This region is meant to characterise a structural system subject to global collapse. Traditionally, it refers to the side-sway mode of collapse, which can be captured via numerical non-convergence on a rigorous mathematical model that takes into account both material and geometric nonlinearities (i.e. it properly simulates collapse Chandramohan et al. (2015)). Numerical non-convergence implies practically infinite *EDP* demand (i.e. $EDP=\infty$), which on the IDA plane is expressed through a characteristic flattening of the IDA curves (Fig. 4(a)). Since demand is practically infinite, seismic fragility can also be obtained by considering an arbitrarily large deterministic *EDP* capacity, i.e. well beyond the last non-collapsing *EDP* value observed in the analysis (e.g. θ_{max}=10%), as shown in Fig. 4(a). The estimation is straightforward and can be performed either on an *EDP* or an *IM*-basis. The conceptual difference of the two approaches appears on Fig. 4(b), where the *EDP*|*IM* as well as the *IM*|*EDP* capacities are presented on four arbitrarily selected single-record IDAs.

A possible complication appears whenever (dense) stripes of *EDP*|*IM* are not available and some form of regression may be required, as often happens with cloud or 2-stripe analysis. Infinite (or just overly large) *EDP* values would make this regression impossible, and the total probability theorem should be invoked to evaluate seismic fragility. This approach combines the event that "the structural capacity is less than the associated seismic demand" with the mutually exclusive events of "*Collapse*" (*Col*) and "*No Collapse*" (*NCol*):

$$F_{LS}(IM) = \mathrm{P}[EDP > EDP_C \mid NCol, IM](1 - \mathrm{P}[Col \mid IM]) + 1 \cdot \mathrm{P}[Col \mid IM] \tag{13}$$

Apparently, the term P[$EDP > EDP_C \mid Col, IM$] is always going to be equal to "1" for any *EDP* value in the above. Actually, this estimation relies on the definition of two functions (Shome 1999), namely the fragilities of collapsing and non-collapsing data, which can be estimated using a logistic regression or the maximum likelihood method (Baker 2015) to handle the sparse collapse data of cloud or few-stripe analysis.

Uncertain EDP capacity

An accurate estimation of the probability of exceedance can only be achieved when capacity is treated as an uncertain variable. At this point one may argue that an elegant estimation of the EDP_C distribution is not possible without a series of large-scale experiments, and thus the uncertain capacity approach should not be adopted in case such information is missing. Obviously, despite the number of laboratory tests performed to estimate various *EDP* capacities of different structural systems (e.g. Lignos et al. (2011)), there is always going to be lack of information as specific setups only have/can be tested. In absence of test data, one could employ, for example, the FEMA P-58 (FEMA 2012) approach to assign a dispersion to an assumed normal or lognormal EDP_C distribution. Either way, the analysis task is complicated as the index (i.e. binary result) functions I[$EDP^j > EDP_C$] and I[$IM > IM_C^j$] now become full distributions (i.e. P[$EDP^j > EDP_C$] and P[$IM > IM_C^j$]), thus requiring one more level of integration (or summation for discrete results) to determine fragility.

EDP-basis estimation

Undoubtedly, inflating EDP_C with a certain amount of variability provides the full picture of the fragility assessment problem. In this case, a sample of equiprobable EDP_C data points is generated (i.e. EDP_C^k, k=1... N_C) via stratified sampling to achieve good resolution/fidelity with only a few (10-20) points, as shown in Fig. 5(a). Therein, the stratified sample of size N_C=10 follows a lognormal distribution that has a median of θ_{max}=2% and dispersion β_{EDPc}=0.3. The probability of exceedance for the uncertain capacity *EDP*-basis approach is also estimated using Eq. (11), only now a MCS is required to take into account the EDP_C distribution effect. The nested "*for-loop*" presented below provides the probability of exceedance for every given *IM*:

```
for every IM level
    estimate demand EDP^j for each record j
    for every EDP_C^k
        estimate F_LS^k(IM) via Eq. (14)
    end for
end for
optionally, combine F_LS^k(IM) to derive F_LS (IM) via Eq. (15)
```

$F_{LS}^k(IM)$ is the fragility of *LS* for a deterministic EDP_C^k capacity.

$$F_{LS}^k(IM) = \frac{\sum_{j=1}^{Nrec} \mathrm{I}\left[EDP^j > EDP_C^k \mid IM\right]}{N_{rec}} \tag{14}$$

$$F_{LS}(IM) = \frac{\sum_{k=1}^{Nc} F_{LS}^k(IM)}{N_C} = \frac{\sum_{k=1}^{Nc}\sum_{j=1}^{Nrec} \mathrm{I}\left[EDP^j > EDP_C^k \mid IM\right]}{N_C N_{rec}} \tag{15}$$

The output of this rather simple algorithm is summarised in Fig. 5(b), where k=1…N_C equally probable fragility curves are formed based on discrete probability data points corresponding to the k^{th} value of *EDP* capacity, EDP_C^k. Those individual fragility curves F_{LS}^k (*IM*) (with median *IM* capacity $IM^k_{C,50\%}$) offer the ability to properly propagate uncertainty to the remaining components of the PBEE framework. In particular, for the assessment of different groups of buildings built to similar standards/materials or by the same contractor or during the same era, same degree of correlation in their EDP_C is to be expected. Correlation among them is very important and must be preserved throughout the limit state MAF/loss estimation. Alternatively, the individual fragility curves can be summarised back into a single CDF by performing an additional summation over the number of the capacities considered via Eq. . This approach is considerably simpler with respect to the MAF estimation, on the offset that provides a rather “smeared” representation of dispersion that contains both the record-to-record and the uncertain capacity component. Selecting between the “discrete” and the “smeared” fragility representation of Eq. (14) and respectively, wholly depends on the needs of the respective user. In most cases, it is the smeared approach that is used, sometimes simply due to lack of correlation information. Other sources of uncertainty, e.g. in the model itself, can be treated in the very same manner by simply differentiating more equiprobable realisations/scenarios than just the k=1…N_C needed for capacity.

IM-basis estimation

The notion of the probabilistic capacity also requires a similar modification/extension for the *IM*-basis methodology. As with the case of the *EDP*-basis procedure, the equiprobable *EDP* capacity data points generated via a stratified sampling are considered. Fig. 6(a) presents the entire set of *IM* capacities for the aforementioned EDP_C sample, and Fig. 6(b) the associated fragility curves. The fragility estimation procedure is nearly identical to the *EDP*-basis approach. The sole difference lies in the MCS procedure, where Eq. (12) is used instead to estimate the discrete probabilities of exceedance:

for every EDP_C^k
    estimate capacities IM_C^{jk} for each record j
    for every *IM* level
        estimate $F_{LS}^k(IM)$ via Eq. (16)
    end for

6 end for

7 optionally, combine $F_{LS}{}^{k}(IM)$ to derive $F_{LS}(IM)$ via Eq. (17)

$$F_{LS}{}^{k}\left(IM\right)=\frac{\sum_{j=1}^{Nrec}\mathrm{I}\left[IM > IM_{C}^{jk}\right]}{N_{rec}} \tag{16}$$

$$F_{LS}\left(IM\right)=\frac{\sum_{k=1}^{Nc}F_{LS}^{k}\left(IM\right)}{N_{C}}=\frac{\sum_{k=1}^{Nc}\sum_{j=1}^{Nrec}\mathrm{I}\left[IM > IM_{C}^{jk}\right]}{N_{C}N_{rec}} \tag{17}$$

In essence, this is the empirical CDF of all the $N_C \cdot N_{rec}$ points that appear in Fig. 6(a). Although a comparison between the *EDP* (Fig. 5(b)) and *IM*-basis (Fig. 6(b)) strategies provides identical results for all practical purposes, there are certain advantages when the latter is employed, mostly for limit states very close to the global instability region (see previous discussion).

Analytical approximations through lognormality

How to incorporate uncertainty under lognormality

Customarily, the discrete probability data points are conveniently summarised back into a single continuous CDF. Experience has shown that the capacity as well as the demand of a structural system can be adequately approximated through the lognormal distribution (Cornell et al. 2002; Jalayer 2003; Romão et al. 2011; Shome 1999). It should be noted that the lognormal (or any other) distribution assumption is essentially another source of epistemic uncertainty, the consequence of which can only be determined in comparison with the empirical data, ideally in terms of MAF of *LS* exceedance. In that sense, under the reasonable assumption that all "N_C" discrete fragilities are lognormal, the "smeared" fragility can also be considered lognormal. Obtaining the median (μ_{IM}) for the "smeared" lognormal CDF is fairly straightforward, as it makes perfect sense to place it on the mean of the corresponding $F_{LS}{}^{k}(IM)$ median *IM* capacities, due to the equiprobable sample considered:

$$\mu_{IM} = \frac{\sum_{k=1}^{N_C} \ln IM_{C,50\%}^{k}}{N_C} \tag{18}$$

On the other hand, dispersion is slightly trickier to determine. The total dispersion (β) is estimated through the law of total variance, which can be summarised using the square root sum of squares (SRSS) rule for the $\beta_{IM,intra}$ and $\beta_{IM,inter}$ terms. $\beta_{IM,intra}$ is the mean intra-fragility dispersion, or the mean of the "N_C" discrete fragility dispersions ($\beta_{IM}{}^{k}$), while $\beta_{IM,inter}$ is the inter-fragility dispersion, i.e. the dispersion of the $IM^{k}{}_{C,50\%}$ median capacities:

$$\begin{gathered}\beta = \sqrt{\beta_{IM,intra}^{2} + \beta_{IM,inter}^{2}} \\ \beta_{IM,intra} = \frac{\sum_{k=1}^{N_C} \beta_{IM}^{k}}{N_C} \\ \beta_{IM,inter} = \sqrt{\frac{\sum_{k=1}^{Nc} \left[\ln IM_{C,50\%}^{k} - \mu_{IM}\right]^{2}}{N_C}}\end{gathered} \tag{19}$$

It is important to keep in mind that although the sample fragility curves may reasonably be individually lognormal, a robust prediction regarding the distribution of the entire discrete probability data points is not possible. Eq. (18) and (19) are valid regardless the distribution of the underlying fragilities, yet the assumption that the overall mean and dispersion also define a lognormal distribution cannot be guaranteed. In fact, whenever the dispersion of EDP_C is large enough and the median IDA is distinctly nonlinear (i.e. curved) in shape, there is a good chance that the overall fragility is not strictly lognormal.

Closed-form solutions

As much as the MCS-based non-parametric approaches offer the full picture of the seismic fragility problem, there are several cases where the MCS output is not available, mostly related to its high computational cost. For such cases, seismic fragility can be evaluated based on data that come from cloud or even a few-stripe analysis, where some form of regression is going to be necessary, and thus response is obtained though the well-known power-law fit of Eq. (10). A well-known misconception is that Eq. (10) must apply to the entire range. Instead, one should only fit it in the region of interest around the median EDP_C (Fig. 7). Of course, getting started with regression implies that lognormality becomes sine-qua-non.

EDP-basis estimation

Under the lognormality assumption for both capacity and demand (and thus their ratio), Eq. (2) can be modified to allow for a simpler way of evaluating seismic fragility, where the analysis results can be directly applied without further post-processing:

$$F_{LS}(IM) = \mathrm{P}[EDP > EDP_C \mid IM] = \mathrm{P}[EDP(IM) > EDP_C] = \mathrm{P}\left[\ln\left(\frac{EDP(IM)}{EDP_C}\right) > \ln 1\right] = \Phi\left(\frac{\ln EDP(IM)_{50\%} - \ln EDP_{C,50\%}}{\beta_{EDP(IM),tot}}\right) \quad (20)$$

Although from a mathematical point of view Eq. (20) is not strictly a “closed-form solution”, in the sense that the CDF cannot be directly obtained through a single formula in its entirety unless several *IM* levels are separately examined, it still presents the closest relationship one may derive through the *EDP*-basis methodology. Its final output suggests that in order to construct a fragility curve, the median capacity and demand estimates are required along with their associated dispersion ($\beta_{EDP(IM),tot}$), for every *IM* level considered. The latter is essentially the ratio of two lognormal distributions which may be obtained through the SRSS rule of their individual (aleatory $\beta_{EDP(IM)}$ and epistemic β_{EDPc}) dispersions, provided that demand and capacity are assumed uncorrelated (see also Cornell et al. (2002); Kazantzi et al. (2014) for additional discussion on capacity-demand correlation):

$$\beta_{EDP(IM),tot} = \sqrt{\beta^2_{EDP(IM)} + \beta^2_{EDPc}} \quad (21)$$

Where negative correlation between demand and capacity exists, implying that easily damageable components will increase structural demand, means that a term of twice the covariance needs to be included under the root, increasing the uncertainty effect (Cornell et al. 2002). The same effect can be accurately incorporated via appropriate sampling and additional dynamic analyses for the earlier parametric approaches (Kazantzi et al. 2014). The aleatory variability around the median demand is clearly a function of the seismic intensity, as denoted through the $\beta_{EDP(IM)}$ term, and as a result it can only be explicitly estimated though IDA (or multi-stripe analysis). For other cases, where a power-law fit is required to define the *EDP-IM* relationship (e.g. cloud, few stripes), the homoscedasticity assumption (i.e. $\beta_{EDP(IM)} = \sigma_{\ln\varepsilon}$, Eq. (10)) is necessary, at least in the local region of EDP_C, to define the entire fragility curve.

Fig. 8(a) provides a comparison of the *EDP*-basis methods presented so far for the "smeared" fragility. An excellent agreement is observed between all approaches, namely the (a) pure MCS approach of Eq. , (b) its lognormal fit via Eq. (18) and (19), (c) the direct application of Eq. (20) and (21) on the raw IDA data, and (d) on the power-law fit. The only problem appears for the latter two cases when *IM* exceeds 0.3g, where the first collapsing record appears. Strictly speaking, $\beta_{EDP(IM)}$ becomes undefined and the distribution of $EDP|IM$ is no longer lognormal. There is a number of tricks one may employ to extend the fragility curves to higher *IM* levels. For instance, case (d) employs the power-law fit to artificially extend the validity of lognormality, by assuming constant dispersion. Regarding case (c), one may extend the fragility up to the *IM* where 16% of ground motion records collapse, employing the $EDP_{84\%}$ and $EDP_{16\%}$ percentiles to estimate the dispersion. By the same logic, one may even use the $EDP_{84\%}$- $EDP_{50\%}$ percentiles, which is valid for cases where the number of collapsing records does not exceed 50% of the ground motions considered. Still, there is a point where all such tricks will fail as $EDP|IM$ is no longer lognormal. At this point, one can employ lognormality only for the non-collapsing records and introduce collapse via Eq. (13), even though, strictly speaking, the non-collapsing points are not exactly lognormal. Maximum likelihood may also be employed to fit a "best-guess" lognormal fragility at higher *IM* levels based on lower *IM* results. In general, employing Eq. (20) on an *EDP*-basis can become challenging due to collapse; yet, it allows to offer the simplest expression of fragility on an *IM*-basis later on.

IM-basis estimation

Combining Eq. (10) and (20) results in the *IM*-basis closed-form solution. This approach finds great application in practice as the probability of exceedance estimation is directly related to the seismic intensity and the prescribed median *EDP* capacity:

$$\begin{aligned} F_{LS}(IM) &= \Phi\left(\frac{\ln\left(aIM^{b}\right) - \ln EDP_{C,50\%}}{\beta_{EDP(IM),tot}}\right) = \Phi\left(\frac{\ln a + b\ln IM - \ln EDP_{C,50\%}}{\beta_{EDP(IM),tot}}\right) \\ &= \Phi\left(\frac{\ln IM - \ln\left[\left(\frac{EDP_{C,50\%}}{a}\right)^{1/b}\right]}{\beta_{EDP(IM),tot}/b}\right) = \Phi\left(\frac{\ln IM - \ln IM_{C,50\%}}{\beta_{IM,tot}}\right) \end{aligned} \tag{22}$$

The associated dispersion ($\beta_{IM,tot}$) is also estimated according to Eq. (21), only this time it incorporates the slope of the underlying power-law approximation:

$$\beta_{IM,tot} = \frac{1}{b}\sqrt{\beta_{EDP(IM)}^{2} + \beta_{EDPc}^{2}} = \sqrt{\beta_{IM|EDP}^{2} + \frac{\beta_{EDPc}^{2}}{b^{2}}} \tag{23}$$

Note that the influence of "*b*" is often neglected in many simplifying approaches that silently assume b=1. As much as this assumption may be valid for moderate-to-long period structures, it is clearly not the case for limit states in the proximity of the global instability region. Yet, it is offset by the fact that little information might be available on each β to begin with.

A comparison of the *IM*-basis closed-form solution versus the "smeared" fragility curve (Eq. (17)), its corresponding lognormal fit (Eq. (18) and (19)) and the empirical CDF obtained for the MCS raw data is presented on Fig. 8(b). The good agreement among those curves not only confirms the results obtained from the *IM*-basis closed-form solution, but also highlights the robustness of the *IM*-basis over the *EDP*-basis approach. This is mainly due to the application of Eq. (22) on the raw IDA data, where the aleatory dispersion is now conditioned on the *EDP* capacity (i.e. $\beta_{IM|EDP}$) rather than the *IM* (i.e. $\beta_{EDP(IM)}$), and thus the infinite *EDP* of collapsing records does not cause any issues.

Limitations regarding the applicability of the aforementioned closed-form solutions exist, and are mostly related to the extent that the power-law approximation is valid for the nonlinear response of a structure. In the general case, the limit state under investigation should be away from the global instability region, as the regression parameters (a, b) cannot be accurately estimated. Eq. (22) may also be adopted for higher states of structural damage where only a certain low percentage of collapsing records ($\leq$ 10%) is observed, however, the latter constitutes a “grey-zone” (due to the “allowable” number of collapsing records) and should be avoided unless special care on estimating the median capacity and the corresponding dispersion is exercised.

General remarks on the lognormality assumption

The lognormal representation of fragility forms a two-parameter model with respect to the median IM_C and its associated dispersion. Various techniques such as the maximum likelihood estimation and the moment-matching approach may be adopted to define the aforementioned parameters. Empirical evidence has shown that the lognormality assumption presents a good fit on the associated data, although one may find cases where other distributions may be equally good or sometimes even better.

Regardless of the *LS* being fit, lognormality means that there is always a non-zero probability that *LS* is violated for an arbitrarily low $IM > 0$. In general, this is not a problem when discussing a structural system on its own, as this is probably negligible (and monotonically decreases very quickly with decreasing *IM*). It becomes quite important though, when applying this fragility to characterize a whole class or group of buildings, like in the case of regional or portfolio loss assessment. Then, when high-damage (e.g. “*near Collapse*” or

"*Collapse*") limit states are discussed, it is possible to find that due to this low probability, over a population of buildings some will collapse even at, say, a *PGA*=0.01g, which is obviously unrealistic. In such cases, one may adopt the empirical CDF that clearly does not suffer from such issues, or if a compact representation is still required, employ a 3-parameter shifted lognormal model, wherein a low $IM_o > 0$ is identified, e.g. at/or below the first *IM* that is found to cause the *LS* violation in the discrete set of analysis runs. The lognormal fitting may then be performed on the shifted IM-IM_o data, instead of just *IM*, where obviously non-positive values are discarded. Henceforth, when a lognormal approximation is discussed, either of the two or three-parameter models are implied as their use is interchangeable, by simply exchanging *IM* with IM-IM_o (Stoica et al. 2007).

Multi-EDP Limit States

So far, the discussion regarding seismic fragility is well-confined under the assumption that the global response can be adequately represented through a single failure mode and *EDP*. Although this approach is valid for most limit states and structural systems of interest, there are several cases where multiple *EDPs* may be needed to determine the violation of a system limit state. For instance, global collapse may be triggered due to global lateral instability, a "simulated" mode of collapse checked via θ_{max}, or due to other modes of failure (e.g. column shear or axial failure) that are often not explicitly modelled ("non-simulated"), either for simplicity or due to the inability to accurately model their effect on the global behaviour (D'Ayala et al. 2015; FEMA 2009; Raghunandan et al. 2015). In such cases, the probability of exceedance should be estimated as

$$F_{LS}(IM) = \mathrm{P}\left[\left(EDP_1 > EDP_{1,C} \mid IM\right) \cup \ldots \cup \left(EDP_m > EDP_{m,C} \mid IM\right)\right], \qquad (24)$$

where *m* is the number of *EDPs* and associated failure modes, each of which may individually trigger the limit state violation. EDP_i denotes the demand and $EDP_{i,C}$ (i=1…m) the capacity.

The case of multiple *EDPs* or failure modes may appear even in more mundane cases that one often associates with a single *EDP*. Perhaps, the most prominent is the case where θ_{max} is used to determine *any* limit state exceedance for a building. Ideally, one should employ the individual storey drifts (θ_i, i=1…m), to check for exceedance at each storey. Using θ_{max} instead, is a useful convention that speeds up computations; yet, is it accurate? Fig. 9(a) illustrates the potential component and system-level approaches that can be used for the seismic fragility evaluation of an m-storey moment resisting frame. The system-level approach is presented on the right side of the vertical dashed line, where the system *EDP* capacity and demand PDFs are shown in terms of θ_{max}. For a given *IM* level, there is a distribution for each θ_i demand and a corresponding distribution for each storey-capacity, as shown by the relevant PDFs appearing on the "component" panels of Fig. 9(a). The distribution of θ_{max} demand is easy to derive in a MCS setting as $\theta_{\max} = \max_i(\theta_i)$; however, the distribution of capacity is not as obvious to estimate from the individual storeys, unless one assumes identical capacities along the height without any correlation. Ideally, both approaches should result in the same system fragility; yet this is not the case unless (a) a single storey dominates the θ_{max} response or (b) all storey capacities are deterministic and of the same value. In the latter case, when capacities are not equal (but still deterministic), one may still employ the demand-to-capacity ratio (*DCR*, Jalayer et al. (2007)) and rewrite each term of Eq. (24) as P[$EDP_i/EDP_{i,C}$>1 | *IM*] to use the maximum demand-capacity ratio of all storeys (or components or failure modes) for simplicity. However, in the more general case where storey (or component)-level capacities are considered uncertain, an MCS should be employed, preferably using the following nested '*for-loop*':

for every *IM* level

    for every storey (or component) i and storey (or component)-level capacity $EDP_{i,C}^k$

        estimate $F_{LS}^k(IM)$ via Eq. (25)

    end for

5 end for

6 optionally, combine $F_{LS}{}^{k}(IM)$ to derive $F_{LS}\,(IM)$ via Eq. (26)

$$F_{LS}^{k}\left(IM\right)=\frac{\sum_{j=1}^{Nrec}\mathrm{I}\left[\text{any}\left(EDP_{i}^{j}>EDP_{i,C}^{k}\right)\mid IM\right]}{N_{rec}} \tag{25}$$

$$F_{LS}\left(IM\right)=\frac{\sum_{k=1}^{Nc}\sum_{j=1}^{Nrec}\mathrm{I}\left[\text{any}\left(EDP_{i}^{j}>EDP_{i,C}^{k}\right)\mid IM\right]}{N_{C}N_{rec}} \tag{26}$$

Fig. 10(a) presents a comparison between the component and system-level fragility curves for the 12-storey case study adopted. When the component-level approach is employed via Eq. (26) and storey capacities are considered uncorrelated, the fragility curve develops a significant shift towards smaller *IM* values compared to the corresponding system-level solution offered via Eq. (15). On the other hand, perfect correlation among different storey capacities results in a perfect match among the aforementioned approaches. Along these lines, it should be noted that when loss estimation via component (FEMA 2012) rather than building-level (D'Ayala et al. 2015) approaches is sought, one does not need to combine such component (or storey)-level fragilities into one, but use them individually to assess the loss of each component.

Another good example to highlight the importance of the "multi-*EDP*" procedure is the case of some industrial structures. The complex response of such structural systems during earthquakes may result into several modes of failure that correspond to varying degrees of loss. The system damage state classification follows an increasing severity pattern that takes into account the leakage potential of the stored materials (Vathi et al. 2017), and requires careful combination of the component-level failure modes in order to assess the functional state of the system (Bakalis et al. 2017). For instance, leakage on a liquid storage tank could be triggered either due to the so-called elephant's foot buckling or to extreme base plate plastic rotations. Similarly, severe structural damage without leakage could be developed both on the base plate due to uplift and the roof of the tank due to sloshing of the contained liquid (Fig. 9(b)). None of these limit states can be described by the same *EDP*, and therefore they are often combined to assess the system-level state of damage.

Since multi-*EDP* fragilities may often be of such practical interest, the simplest scenario of two failure modes (e.g. A, B) controlling a single *DS* is further presented. In the general case, one needs to account for correlation of demands EDP_A, EDP_B and capacities $EDP_{A,C}$, $EDP_{B,C}$ via MCS. Hence, Eq. (24) may be expanded accordingly:

$$
\begin{gathered}
F_{LS}(IM) = F_{LS}^{A}(IM) + F_{LS}^{B}(IM) - F_{LS}^{A\cap B}(IM) \\
F_{LS}^{A}(IM) = \frac{\sum_{j=1}^{Nrec} \mathrm{P}\left[EDP_A^j > EDP_{A,C} \mid IM\right]}{N_{rec}} = \frac{\sum_{k=1}^{Nc}\sum_{j=1}^{Nrec} \mathrm{I}\left[EDP_A^j > EDP_{A,C}^k \mid IM\right]}{N_C N_{rec}} \\
F_{LS}^{B}(IM) = \frac{\sum_{j=1}^{Nrec} \mathrm{P}\left[EDP_B^j > EDP_{B,C} \mid IM\right]}{N_{rec}} = \frac{\sum_{k=1}^{Nc}\sum_{j=1}^{Nrec} \mathrm{I}\left[EDP_B^j > EDP_{B,C}^k \mid IM\right]}{N_C N_{rec}} \\
F_{LS}^{A\cap B}(IM) = \frac{\sum_{k=1}^{Nc}\sum_{j=1}^{Nrec} \mathrm{I}\left[EDP_A^j > EDP_{A,C}^k \cap EDP_B^j > EDP_{B,C}^k \mid IM\right]}{N_C N_{rec}}
\end{gathered}
\tag{27}
$$

Eventually, the only practical difficulty may lie in estimating the probability of the intersection of the events *A* and *B*. For the case that the two capacities are independent (demands are usually correlated), the intersection can be estimated for each ground motion record through the product of the individual probabilities as:

$$
F_{LS}^{A\cap B}(IM) = \frac{\sum_{j=1}^{Nrec} \mathrm{P}\left[EDP_A^j > EDP_{A,C} \mid IM\right] \cdot \mathrm{P}\left[EDP_B^j > EDP_{B,C} \mid IM\right]}{N_{rec}} \tag{28}
$$

Fig. 10(b) depicts the fragility curves for events *A* and *B*, their intersection and the associated union based on Eq. (27) and (28).

Conclusions

A comprehensive overview on existing seismic fragility functions has been presented for methods that rely on nonlinear dynamic analysis. A 12-storey moment resisting frame has been adopted to illustrate the various methodologies that can be used to extract fragility curves. As expected, the *EDP*-basis results match the ones generated though the *IM*-basis approach, both under a deterministic and an uncertain *EDP* capacity framework. Although *EDP*-basis is easier to digest compared to the slightly trickier *IM*-basis, the latter presents a more robust probability of exceedance estimation approach, especially for limit states close to the global instability region. The aforementioned methodologies can be used to evaluate the system fragility of a structural system using a single global *EDP*, or take a step further and employ local *EDPs* and failure modes to allow for higher resolution in a complex system-fragility estimation. Undeniably, seismic assessment procedures based on system-level response parameters have dominated standard practice. Recent advances, however, point towards the use of component-level approaches for the damage and loss estimation of single structures, delegating system-level fragility only to the role of estimating collapse or demolition potential. Even so, regional and portfolio assessment remains grounded on system fragility estimates, leaving ample space for applications.

References

ASCE. (2007). *Seismic Rehabilitation of Existing Buildings*. American Society of Civil Engineers, ASCE Standard ASCE/SEI 41-06.

ATC. (1985). *Earthquake Damage Evaluation Data for California, Report No. ATC-13*. Applied Technology Council, Redwood City, CA.

Bakalis, K., Vamvatsikos, D., and Fragiadakis, M. (2017). "Seismic risk assessment of liquid storage tanks via a nonlinear surrogate model." *Earthquake Engineering & Structural Dynamics*, 46(15), 2851–2868.

Baker, J. W. (2015). "Efficient Analytical Fragility Function Fitting Using Dynamic Structural Analysis." *Earthquake Spectra*, 31(1), 579–599.

Baker, J. W., and Cornell, C. A. (2006). "Spectral shape, epsilon and record selection." *Earthquake Engineering and Structural Dynamics*, 35(9), 1077–1095.

Bazzurro, P., and Cornell, C. A. (2002). "Vector-Valued Probabilistic Seismic Hazard Analysis (VPSHA)." *Proceedings of the 7th U.S. National Conference on Earthquake Engineering*, Boston, Massachusetts, USA.

Bazzurro, P., Cornell, C. A., Menun, C., Motahari, M., and Luco, N. (2006). *Advanced seismic assessment guidelines*. PEER Report No. 2006/05, Pacific Earthquake Engineering Research Center, University of California, Berkeley, CA.

Bazzurro, P., Cornell, C. A., Shome, N., and Carballo, J. E. (1998). "Three Proposals for Characterizing MDOF Nonlinear Seismic Response." *Journal of Structural Engineering*, 124(11), 1281–1289.

Bradley, B. A. (2011). "Correlation of Significant Duration with Amplitude and Cumulative Intensity Measures and Its Use in Ground Motion Selection." *Journal of Earthquake Engineering*, 15(6), 809–832.

Chandramohan, R., Baker, J. W., and Deierlein, G. G. (2015). "Impact of computational choices on estimated structural collapse capacity under earthquake ground motions." *Engineering Mechanics Institute Conference 2015*.

Cordova, P., Deierlein, G., Mehanny, S. F., and Cornell, C. A. (2001). "Development of a two-parameter seismic intensity measure and probabilistic design procedure." *The Second U.S.- Japan Workshop on Performance-Based Earthquake Engineering Methodology for Reinforced Concrete Building Structures*, Sapporo, Hokkaido, 187–206.

Cornell, C. A., Jalayer, F., Hamburger, R. O., and Foutch, D. (2002). "Probabilistic Basis for 2000 SAC Federal Emergency Management Agency Steel Moment Frame Guidelines." *Journal of Structural Engineering*.

Cornell, C. A., and Krawinkler, H. (2000). "Progress and Challenges in Seismic Performance Assessment." *PEER Center News*, 3(2), 1–4.

D'Ayala, D., Meslem, A., Vamvatsikos, D., Porter, K., and Rossetto, T. (2015). *Guidelines for Analytical Vulnerability Assessment - Low/Mid-Rise Buildings*. Vulnerability Global Component Project.

Deierlein, G. G., Krawinkler, H., and Cornell, C. A. (2003). "A framework for performance-based earthquake engineering." *7th Pacific Conference on Earthquake Engineering*, Christchurch, New Zealand.

Dolsek, M. (2009). "Incremental dynamic analysis with consideration of modeling uncertainties." *Earthquake Engineering & Structural Dynamics*, 38(6), 805–825.

Eads, L., Miranda, E., and Lignos, D. (2016). "Spectral shape metrics and structural collapse potential." *Earthquake Engineering & Structural Dynamics*, 45(10), 1643–1659.

Ellingwood, B. R., and Kinali, K. (2009). "Quantifying and communicating uncertainty in seismic risk assessment." *Structural Safety*, Elsevier Ltd, 31(2), 179–187.

FEMA. (2009). *Quantification of Building Seismic Performance Factors*. FEMA P-695, prepared by Applied Technology Council for Federal Emergency Management Agency, Washington, D.C.

FEMA. (2012). *Seismic Performance Assessment of Buildings*. FEMA P-58, prepared by the Applied Technology Council for the Federal Emergency Management Agency, Washington D.C.

Fragiadakis, M., Vamvatsikos, D., and Aschheim, M. (2014). "Application of Nonlinear Static Procedures for the Seismic Assessment of Regular RC Moment Frame Buildings." *Earthquake Spectra*, 30(2), 767–794.

Gidaris, I., Padgett, J. E., Barbosa, A. R., Chen, S., Cox, D., Webb, B., and Cerato, A. (2017). "Multiple-Hazard Fragility and Restoration Models of Highway Bridges for Regional Risk and Resilience Assessment in the United States: State-of-the-Art Review." *Journal of Structural Engineering*, 143(3), 4016188.

Goulet, C. A., Haselton, C. B., Mitrani-Reiser, J., Beck, J. L., Deierlein, G. G., Porter, K. A., and Stewart, J. P. (2007). "Evaluation of the seismic performance of a code-conforming reinforced-concrete frame building—from seismic hazard to collapse safety and economic losses." *Earthquake Engineering & Structural Dynamics*, 36(13), 1973–1997.

Jaiswal, K., Wald, D., and D'Ayala, D. (2011). "Developing Empirical Collapse Fragility Functions for

Global Building Types." *Earthquake Spectra*, 27(3), 775–795.

Jalayer, F. (2003). "Direct Probabilistic Seismic Anaysis: Implementing Non-linear Dynamic Assessments." Ph.D. dissertation, Dept. of Civil and Environmental Engineering, Stanford Univ., Stanford, CA.

Jalayer, F., and Cornell, C. A. (2009). "Alternative non-linear demand estimation methods for probability-based seismic assessments." *Earthquake Engineering & Structural Dynamics*, 38(8), 951–972.

Jalayer, F., Franchin, P., and Pinto, P. E. (2007). "A scalar damage measure for seismic reliability analysis of RC frames." *Earthquake Engineering & Structural Dynamics*, 36(13), 2059–2079.

Kazantzi, A. K., and Vamvatsikos, D. (2015). "Intensity measure selection for vulnerability studies of building classes." *Earthquake Engineering & Structural Dynamics*, 44(15), 2677–2694.

Kazantzi, A. K., Vamvatsikos, D., and Lignos, D. G. (2014). "Seismic performance of a steel moment-resisting frame subject to strength and ductility uncertainty." *Engineering Structures*, 78, 69–77.

Kennedy, R. P., and Ravindra, M. K. (1984). "Seismic fragilities for nuclear power plant risk studies." *Nuclear Engineering and Design*, 79(1), 47–68.

Der Kiureghian, A., and Ditlevsen, O. (2009). "Aleatory or epistemic? Does it matter?" *Structural Safety*, Elsevier Ltd, 31(2), 105–112.

Kohrangi, M., Bazzurro, P., and Vamvatsikos, D. (2016). "Vector and Scalar IMs in Structural Response Estimation, Part II: Building Demand Assessment." *Earthquake Spectra*, 32(3), 1525–1543.

Lallemant, D., Kiremidjian, A., and Burton, H. (2015). "Statistical procedures for developing earthquake damage fragility curves." *Earthquake Engineering & Structural Dynamics*, 44(9), 1373–1389.

Liel, A. B., Haselton, C. B., Deierlein, G. G., and Baker, J. W. (2009). "Incorporating modeling uncertainties in the assessment of seismic collapse risk of buildings." *Structural Safety*, Elsevier Ltd, 31(2), 197–211.

Lignos, D. G., Krawinkler, H., and Whittaker, A. S. (2011). "Prediction and validation of sidesway collapse of two scale models of a 4-story steel moment frame." *Earthquake Engineering &*

Structural Dynamics, 40(7), 807–825.

Luco, N., and Bazzurro, P. (2007). “Does amplitude scaling of ground motion records result in biased nonlinear structural drift responses?” *Earthquake Engineering & Structural Dynamics*, 36(13), 1813–1835.

Luco, N., and Cornell, C. A. (2007). “Structure-Specific Scalar Intensity Measures for Near-Source and Ordinary Earthquake Ground Motions.” *Earthquake Spectra*, 23(2), 357–392.

Mackie, K., and Stojadinovic, B. (2001). “Probabilistic Seismic Demand Model for California Highway Bridges.” *Journal of Bridge Engineering*, 6(6), 468–481.

Miranda, E., and Aslani, H. (2003). *Probabilistic Response Assessment for Building-Specific Loss Estimation*. PEER Report No. 2003/03, Pacific Earthquake Engineering Research Center, University of California, Berkeley, CA.

Mitrani-Reiser, J. (2007). “An Ounce of Prevention: Probabilistic Loss Estimation for Performance-based Earthquake Engineering.” Ph.D. dissertation, Dept. of Civil and Environmental Engineering, California Institute of Technology, Pasadena, CA.

Moehle, J. P., and Deierlein, G. G. (2004). “A Framework for Performance-Based Earthquake Engineering.” *13th World Conference on Earthquake Engineering*, Vancouver, B.C., Canada.

Nielson, B. G., and DesRoches, R. (2007a). “Analytical seismic fragility curves for typical bridges in the central and southeastern United States.” *Earthquake Spectra*, 23(3), 615–633.

Nielson, B. G., and DesRoches, R. (2007b). “Seismic fragility methodology for highway bridges using a component level approach.” *Earthquake Engineering & Structural Dynamics*, 36(6), 823–839.

Noh, H. Y., Lallemant, D., and Kiremidjian, A. S. (2015). “Development of empirical and analytical fragility functions using kernel smoothing methods.” *Earthquake Engineering & Structural Dynamics*, 44(8), 1163–1180.

Padgett, J. E., and DesRoches, R. (2008). “Methodology for the development of analytical fragility curves for retrofitted bridges.” *Earthquake Engineering & Structural Dynamics*, 37(8), 1157–1174.

Porter, K. A. (2015). “A Beginner’s Guide to Fragility, Vulnerability, and Risk.” *University of Colorado Boulder*, <http://spot.colorado.edu/~porterka/Porter-beginners-guide.pdf>.

Porter, K., Mitrani-Reiser, J., and Beck, J. L. (2006). "Near-real-time loss estimation for instrumented buildings." *The Structural Design of Tall and Special Buildings*, 15(1), 3–20.

Raghunandan, M., Liel, A. B., and Luco, N. (2015). "Collapse Risk of Buildings in the Pacific Northwest Region due to Subduction Earthquakes." *Earthquake Spectra*, 31(4), 2087–2115.

Romão, X., Delgado, R., and Costa, A. (2011). "Assessment of the Statistical Distributions of Structural Demand Under Earthquake Loading." *Journal of Earthquake Engineering*, 15(5), 724–753.

Rossetto, T., and Elnashai, A. (2005). "A new analytical procedure for the derivation of displacement-based vulnerability curves for populations of RC structures." *Engineering Structures*, 27(3), 397–409.

Rossetto, T., Ioannou, I., Grant, D., and Maqsood, T. (2014). *Guidelines for empirical vulnerability assessment*. GEM Technical Report 2014-08 V1.0.0, GEM Foundation, Pavia, Itally.

Schotanus, M. I. J., Franchin, P., Lupoi, A., and Pinto, P. E. (2004). "Seismic fragility analysis of 3D structures." *Structural Safety*, 26(4), 421–441.

Shinozuka, M., Feng, M. Q., Lee, J., and Naganuma, T. (2000). "Statistical Analysis of Fragility Curves." *Journal of Engineering Mechanics*, 126(12), 1224–1231.

Shome, N. (1999). "Probabilistic Seismic Demand Analysis Of Nonlinear Structures." Ph.D. dissertation, Dept. of Civil and Environmental Engineering, Stanford Univ., Stanford, CA.

Shome, N., Cornell, C. A., Bazzurro, P., and Carballo, J. E. (1998). "Earthquakes, Records, and Nonlinear Responses." *Earthquake Spectra*, 14(3), 469–500.

Silva, V., Crowley, H., Varum, H., Pinho, R., and Sousa, R. (2014). "Evaluation of analytical methodologies used to derive vulnerability functions." *Earthquake Engineering & Structural Dynamics*, 43(2), 181–204.

Stoica, M., Medina, R. A., and McCuen, R. H. (2007). "Improved probabilistic quantification of drift demands for seismic evaluation." *Structural Safety*, 29(2), 132–145.

Tothong, P., and Cornell, C. A. (2008). "Structural performance assessment under near-source pulse-like ground motions using advanced ground motion intensity measures." *Earthquake Engineering & Structural Dynamics*, 37(7), 1013–1037.

Tsantaki, S., Adam, C., and Ibarra, L. F. (2017). "Intensity measures that reduce collapse capacity dispersion of P-delta vulnerable simple systems." *Bulletin of Earthquake Engineering*, Springer Netherlands, 15(3), 1085–1109.

Vamvatsikos, D., and Cornell, C. A. (2002). "Incremental dynamic analysis." *Earthquake Engineering & Structural Dynamics*, 31(3), 491–514.

Vamvatsikos, D., and Cornell, C. A. (2004). "Applied Incremental Dynamic Analysis." *Earthquake Spectra*, 20(2), 523–553.

Vamvatsikos, D., and Fragiadakis, M. (2010). "Incremental dynamic analysis for estimating seismic performance sensitivity and uncertainty." *Earthquake Engineering & Structural Dynamics*, 39(2), 141–163.

Vathi, M., Karamanos, S. A., Kapogiannis, I. A., and Spiliopoulos, K. V. (2017). "Performance Criteria for Liquid Storage Tanks and Piping Systems Subjected to Seismic Loading." *Journal of Pressure Vessel Technology*, 139(5), 51801.

Wen, Y. K., and Ellingwood, B. R. (2005). "The role of fragility assessment in consequence-based engineering." *Earthquake Spectra*, 21(3), 861–877.

Zareian, F., Ibarra, L., and Krawinkler, H. (2004). "Seismic demands and capacities of single-story and low- rise multi-story woodframe structures." *Proceedings of the 13th World Conference on Earthquake Engineering*, Vancouver, B.C., Canada.

Zeris, C., Vamvatsikos, D., and Giannitsas, P. (2007). "Impact of FE Modeling in the Seismic Performance Prediction of Existing RC Buildings." *ECCOMAS Thematic Conference on Computational Methods in Structural Dynamics and Earthquake Engineering*, Rethymno, Crete Island, Greece, 13–16.

Figure Captions

Fig. 1. (a) Single-record IDA curves and example of $EDP|IM$ and $IM|EDP$ distributions. The shaded areas represent the two alternative approaches in defining the seismic fragility for a deterministic EDP capacity θ_{max}=2%. An $IM|EDP$ vertical stripe at θ_{max}=2% fully defines fragility, while multiple horizontal stripes (here shown at 0.4g) are needed for an equivalent

result. (b) Stripe analysis for the 0.7g and 0.9g *IM* levels and cloud analysis for the unscaled FEMA P-695 (FEMA 2009) ground motion set, together with a power-law fit for the latter.

Fig. 2. EDP-basis approach for deterministic *EDP* capacity: (a) Three illustrative *IM* stripes on the single-record IDA curves. (b) Discrete $F_{LS}(IM)$ results via Eq. (11) and continuous lognormal fit. The filled triangles refer to *IM* levels equal to 0.2g, 0.4g and 0.6g respectively.

Fig. 3. *IM*-basis approach for a deterministic *EDP* capacity: (a) IM_C points and three illustrative horizontal *IM*-demand levels on the single-record IDA curves. (b) Discrete $F_{LS}(IM)$ results via Eq. (12) and continuous lognormal fit. The filled triangles refer to *IM* levels equal to 0.2g, 0.4g and 0.6g respectively.

Fig. 4. (a) Global instability data points on all 44 IDA curves. (b) *EDP*|*IM* and *IM*|*EDP* data points on 4 arbitrary IDA curves, featuring the *EDP* versus *IM*-basis probability of exceedance estimation for a limit state capacity that adequately represents global instability.

Fig. 5. *EDP*-basis approach for uncertain *EDP* capacity: (a) A stratified sample of N_C=10 equiprobable *EDP* capacities and three illustrative *IM* stripes on the single-record IDA curves. (b) Discrete versus smeared fragility curve via Eq. (14) and , respectively.

Fig. 6. *IM*-basis approach for uncertain *EDP* capacity: (a) A stratified sample of N_C=10 equiprobable *EDP* capacities and three illustrative IM stripes on the single-record IDA curves. (b) The N_C=10 discrete versus the smeared fragility curve via Eq. (16) and (17), respectively. Each discrete fragility curve is the CDF of a single vertical stripe of IM_C points.

Fig. 7. Single-record, 16%, 50% and 84% IDA curves, featuring the corresponding local power-law fit for the (θ_{max}=2%, $S_a(T_1)$=0.4g) median capacity point. Elsewhere, the fit may not be valid.

Fig. 8. (a) *EDP*-basis closed-form comparison to MCS “smeared” and lognormal fit fragility curves. (b) *IM*-basis closed-form comparison to MCS “smeared”, lognormal fit and empirical CDF fragility estimates.

Fig. 9. (a) Component versus system-level demand and capacity distribution patterns for the seismic fragility estimation of an uncertain m-storey moment resisting frame. The PDFs of θ_i demand and capacity are presented vis-à-vis the ones of θ_{max} conditioned on the *IM*. (b) Component-level demand and capacity distributions for various failure modes on an unanchored liquid storage tank.

Fig. 10. (a) System versus component-level fragility estimation. The estimation has been performed based on Eq. (15) and (26). (b) Illustrative fragility curve generation example for damage states that depend on two failure modes (or *EDPs*). The estimation has been performed based on Eq. (27) and (28).

Figures

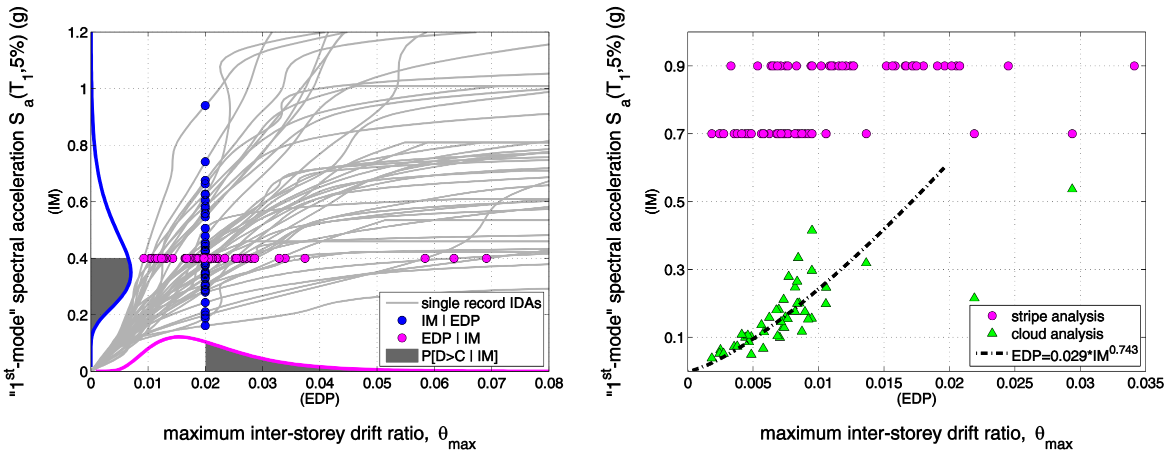

(a) (b)

Fig. 1. (a) Single-record IDA curves and example of *EDP*|*IM* and *IM*|*EDP* distributions. The shaded areas represent the two alternative approaches in defining the seismic fragility for a deterministic *EDP* capacity θ_{max}=2%. An *IM*|*EDP* vertical stripe at θ_{max}=2% fully defines fragility, while multiple horizontal stripes (here shown at 0.4g) are needed for an equivalent result. (b) Stripe analysis for the 0.7g and 0.9g *IM* levels and cloud analysis for the unscaled FEMA P-695 (FEMA 2009) ground motion set, together with a power-law fit for the latter.

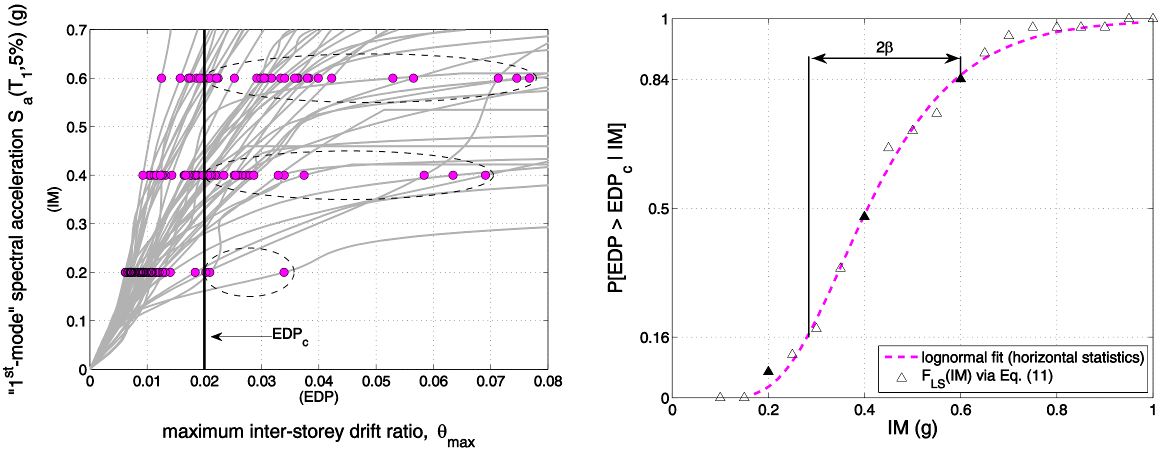

(a) (b)

Fig. 2. EDP-basis approach for deterministic *EDP* capacity: (a) Three illustrative *IM* stripes on the single-record IDA curves. (b) Discrete $F_{LS}(IM)$ results via Eq. (11) and continuous lognormal fit. The filled triangles refer to *IM* levels equal to 0.2g, 0.4g and 0.6g respectively.

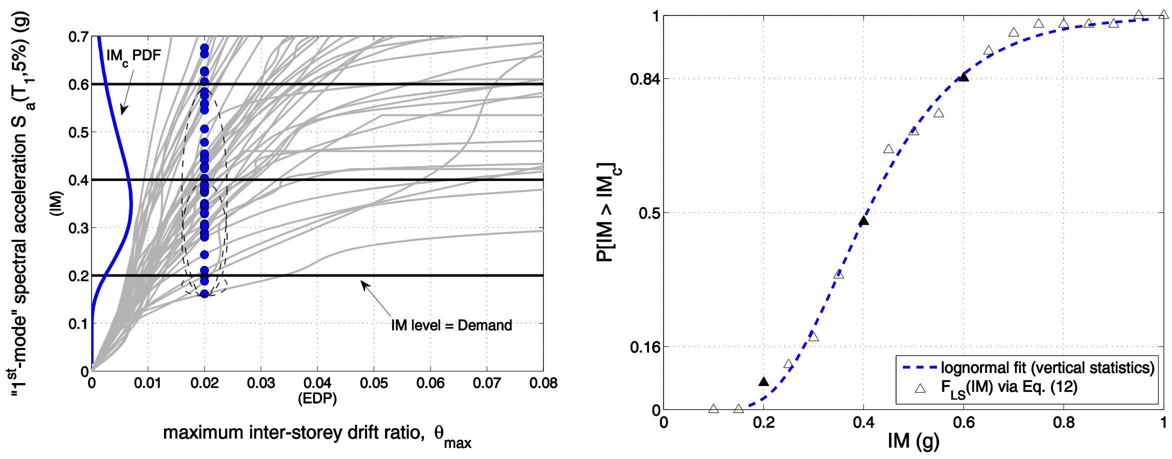

(a) (b)

Fig. 3. *IM*-basis approach for a deterministic *EDP* capacity: (a) IM_C points and three illustrative horizontal *IM*-demand levels on the single-record IDA curves. (b) Discrete $F_{LS}(IM)$ results via Eq. (12) and continuous lognormal fit. The filled triangles refer to *IM* levels equal to 0.2g, 0.4g and 0.6g respectively.

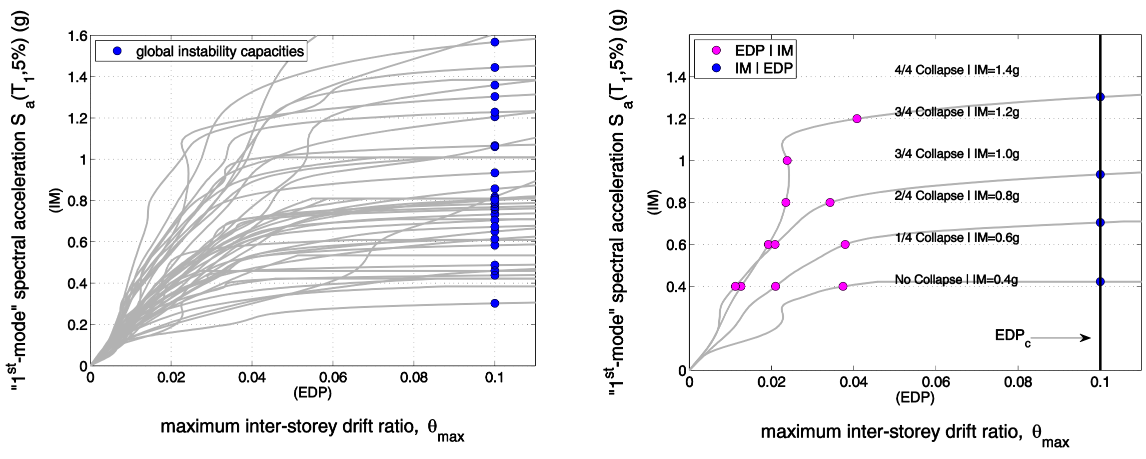

(a) (b)

Fig. 4. (a) Global instability data points on all 44 IDA curves. (b) *EDP*|*IM* and *IM*|*EDP* data points on 4 arbitrary IDA curves, featuring the *EDP* versus *IM*-basis probability of exceedance estimation for a limit state capacity that adequately represents global instability.

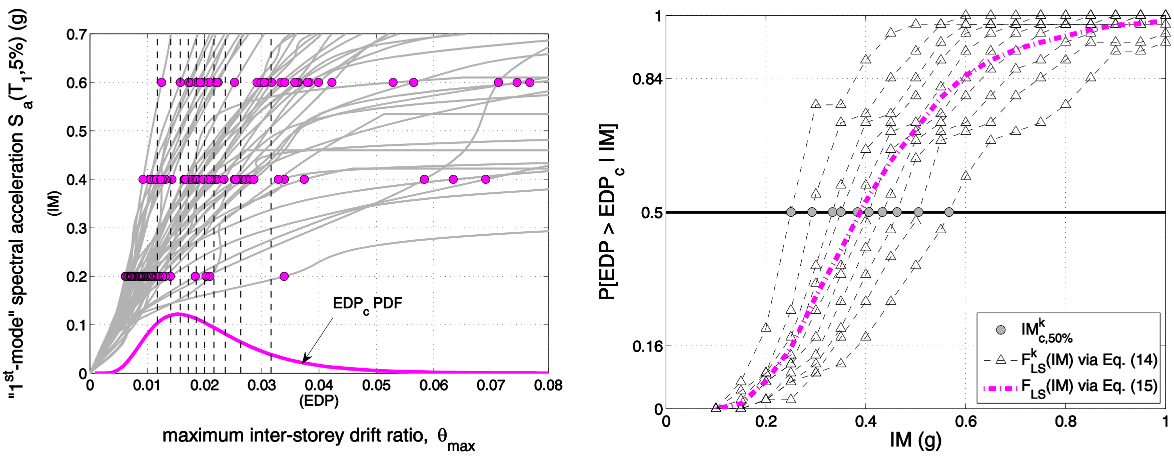

(a) (b)

Fig. 5. *EDP*-basis approach for uncertain *EDP* capacity: (a) A stratified sample of N_C=10 equiprobable *EDP* capacities and three illustrative *IM* stripes on the single-record IDA curves. (b) Discrete versus smeared fragility curve via Eq. (14) and , respectively.

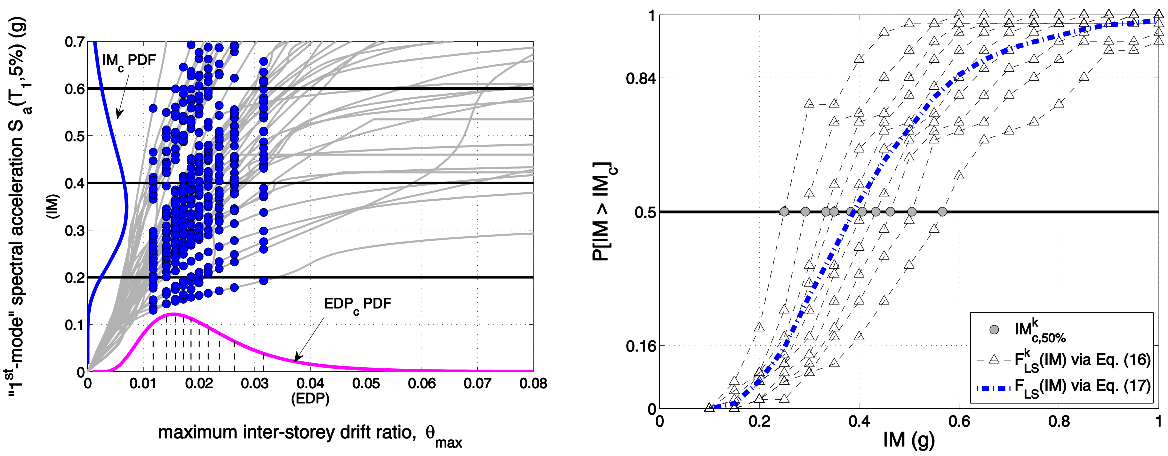

(a) (b)

Fig. 6. *IM*-basis approach for uncertain *EDP* capacity: (a) A stratified sample of N_C=10 equiprobable *EDP* capacities and three illustrative IM stripes on the single-record IDA curves. (b) The N_C=10 discrete versus the smeared fragility curve via Eq. (16) and (17), respectively. Each discrete fragility curve is the CDF of a single vertical stripe of IM_C points.

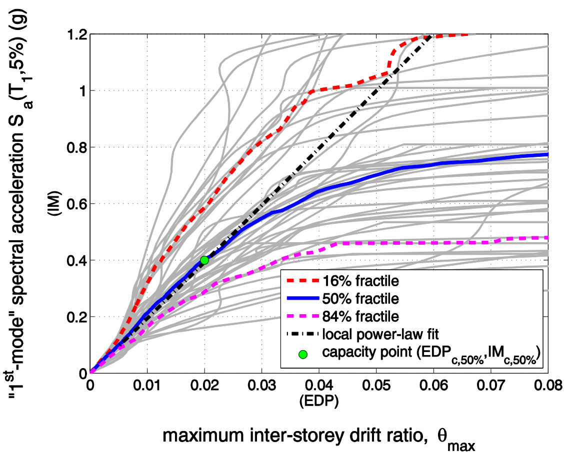

Fig. 7. Single-record, 16%, 50% and 84% IDA curves, featuring the corresponding local power-law fit for the (θ_{max}=2%, $S_a(T_1)$=0.4g) median capacity point. Elsewhere, the fit may not be valid.

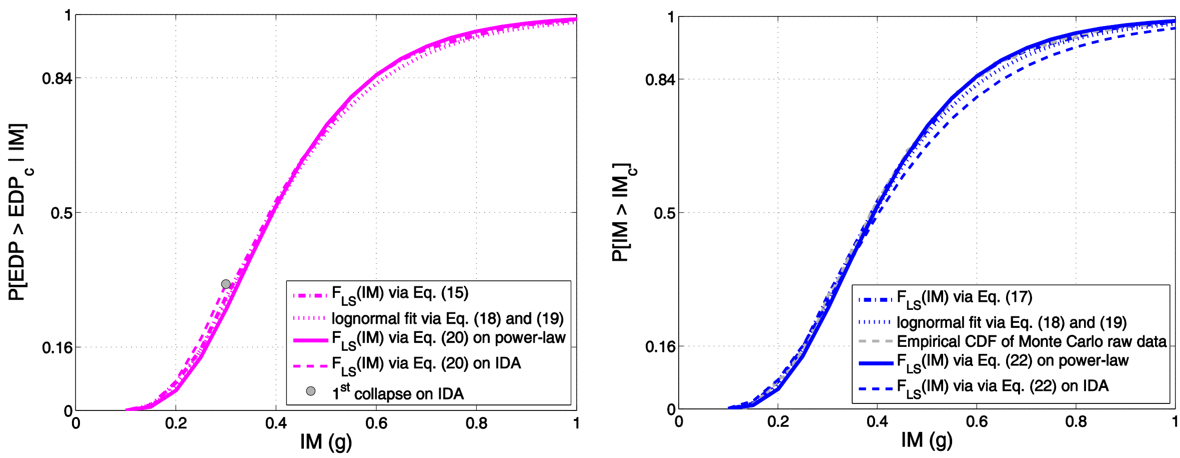

(a) (b)

Fig. 8. (a) *EDP*-basis closed-form comparison to MCS "smeared" and lognormal fit fragility curves. (b) *IM*-basis closed-form comparison to MCS "smeared", lognormal fit and empirical CDF fragility estimates.

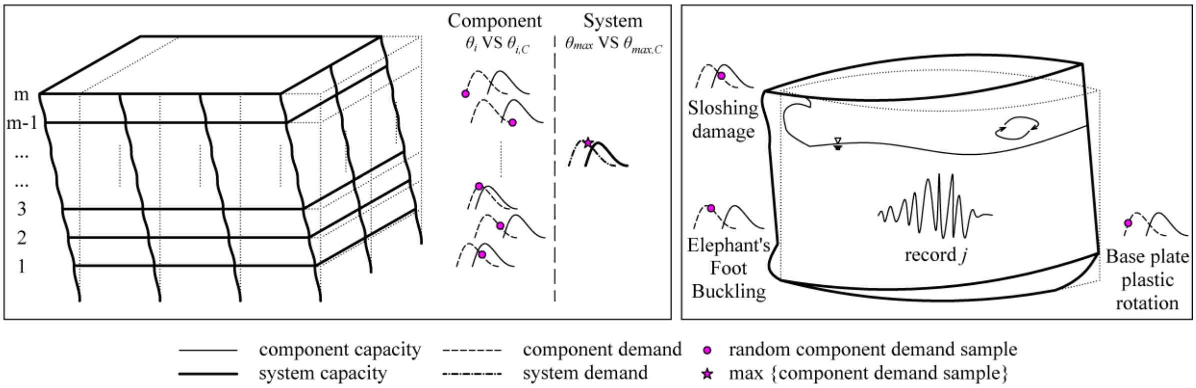

(a) (b)

Fig. 9. (a) Component versus system-level demand and capacity distribution patterns for the seismic fragility estimation of an uncertain m-storey moment resisting frame. The PDFs of θ_i demand and capacity are presented vis-à-vis the ones of θ_{max} conditioned on the *IM*. (b) Component-level demand and capacity distributions for various failure modes on an unanchored liquid storage tank.

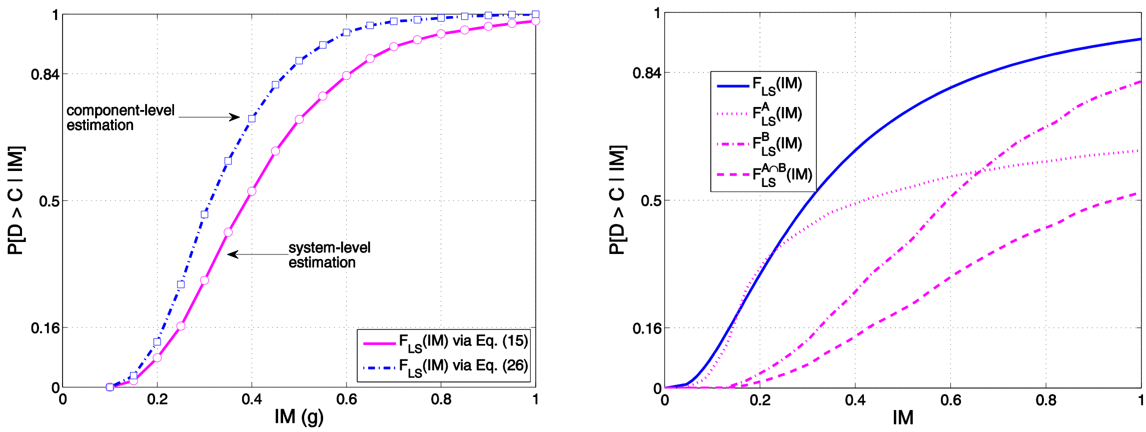

(a) (b)

Fig. 10. (a) System versus component-level fragility estimation. The estimation has been performed based on Eq. (15) and (26). (b) Illustrative fragility curve generation example for damage states that depend on two failure modes (or *EDPs*). The estimation has been performed based on Eq. (27) and (28).